Mechanically gated channel activity in cytoskeleton-deficient plasma membrane blebs and vesicles from *Xenopus* oocytes

Yong Zhang, Feng Gao, Vsevolod L. Popov*, Julie W. Wen* and Owen P. Hamill

*Physiology and Biophysics and *Pathology, University of Texas Medical Branch, Galveston, TX 77555-0641, USA*

(Received 10 June 1999; accepted after revision 10 November 1999)

1. A novel technique involving hypertonic stress causes membrane 'blebbing' of the *Xenopus* oocyte and the shedding of plasma membrane vesicles (PMVs).

2. Confocal fluorescence microscopy, immunocytochemistry and electron microscopy indicate that blebs and PMVs lack cortical cytoskeleton and are deficient in cytoskeleton proteins and devoid of microvilli.

3. Patch recordings from PMVs consistently reveal mechanically gated (MG) channel activity. The MG channels display the same single-channel conductance as control recordings but differ in terms of reduced mechanosensitivity and adaptation to sustained stimulation.

4. Whole PMV recordings show rapid and reversible activation of mechanosensitive currents in response to pressure pulses. The maximal currents activated in PMVs are consistent with MG channel activity recorded in patches.

5. The discrepancy between MG channel activity recorded in whole PMVs and oocytes most probably reflects their different membrane geometry and ability to develop activating bilayer tensions.

6. We propose that membrane blebbing, which is known to occur under specific physiological and pathological conditions (e.g. mitosis and apoptosis), may increase mechanosensitivity independently of the intrinsic properties of membrane proteins.

In our previous studies we were unable to activate whole-cell MG channel currents in *Xenopus* oocytes despite the consistent recording of MG channel activity in patch-clamp recordings (Zhang & Hamill, 2000*a*,*b*). One hypothesis to explain such a discrepancy is that tight seal formation makes the patch hyper-mechanosensitive by disrupting the cortical cytoskeleton that otherwise protects the membrane bilayer (Morris & Horn, 1991; Small & Morris, 1994; Wan *et al.* 1999; see also Hamill & McBride, 1997). A variation on this hypothesis is that the cytoskeleton, by allowing complex membrane geometry, provides an immediate membrane reserve that can buffer tension changes in the bilayer (Zhang & Hamill, 2000*b*). To test the basic hypothesis, it would be useful to examine the biochemistry and structure of the underlying membrane cytoskeleton. However, it is difficult to apply biochemical and electron microscopy techniques to the small membrane patch sealed in the tip of a patch pipette. To circumvent this difficulty we have developed a new plasma membrane preparation from *Xenopus* oocytes involving membrane blebs and isolated plasma membrane vesicles (PMVs). We show that the blebs and PMVs lack cortical cytoskeleton structures, are deficient in cytoskeleton proteins and devoid of microvilli. Furthermore, we use patch-clamp recording to examine the properties of the MG channel currents that can be activated in blebs and PMVs.

METHODS

Xenopus laevis were anaesthetized and oocytes removed. Recovery of the frogs was monitored. Not less than 3 months later a second collection was made after which anaesthetized frogs were decapitated. See Zhang & Hamill (2000*a*) for full details. The care of frogs, preparation of oocytes, solutions, chemicals voltage-clamp, patch-clamp, pressure-clamp and imaging techniques were the same as described in Zhang & Hamill (2000*a*,*b*).

Induction of membrane blebs and vesicles from *Xenopus* oocytes

Oocytes were first placed in stripping solution for ~5 min and the vitelline membrane was removed using fine forceps. The oocytes were then placed in 'blebbing solution' which contained (mM): 400 potassium aspartate, 20 KCl, 10 EGTA, 1 $MgCl_2$ and 10 Hepes-KOH (800 mosmol l^{-1}). After incubating the oocytes for 2 h in this solution, membrane blebs could be seen to form over the entire surface of the oocyte and with additional time many of the blebs detached from the surface of the oocyte to form isolated vesicles.

Immunofluorescence and confocal microscopy

Control oocytes and the hypertonicity-induced blebs and vesicles were examined under confocal microscopy (Odyssey Real Time

Laser Confocal Microscope). NBD phallacidin (NBD-P) and 9-dicyanovinylljulolidin (DCVJ) were added to the incubating solution for 3 h to overnight to stain the actin and tubulin, respectively. In some experiments, NBD-P (1 mM in DMSO) was diluted in 100 mM KCl (100 μM) and directly microinjected into the oocytes to give a final concentration of 10 μM. Similar fluorescent staining of the cortical cytoskeleton was seen with the two procedures. However, in general, microinjected oocytes did not bleb as profusely as uninjected oocytes, possibly due to membrane damage.

Preparation of oocyte homogenate and plasma membrane fractions

Stage V and VI oocytes were treated with collagenase and stored in Barth's solution. The follicular and vitelline membrane layers were manually removed from 100 oocytes which were then homogenized in 2·5 ml of 10% (w/v) sucrose in (mM): 150 NaCl, 10 magnesium acetate, 20 Tris-HCl (pH 7·6), containing phenylmethylsulfonylfluoride. The homogenate (0·5 ml was stored at −20 °C for later protein assay and electrophoresis) was layered on top of a discontinuous sucrose gradient (1·2 ml each of 50% and 20% (w/v) sucrose in (mM): 150 NaCl, 10 magnesium acetate, 20 Tris-HCl, pH 7·4) and centrifuged for 30 min at 15 000 *g* in a Beckman SW 55 rotor. The membrane was collected from the 20–50% sucrose interface, washed once in homogenization buffer without sucrose, resuspended in the same solution and stored at −20 °C.

Preparation of large quantities of PMVs

Large quantities of PMVs were prepared by placing 100–500 stripped oocytes on a nylon mesh in a 60 mm Corning culture dish containing blebbing solution overnight at 19 °C. Care was taken not to include any damaged oocytes. The oocytes were removed and the remaining PMVs collected by high-speed centrifugation (30 000 *g*, for 30 min at 4 °C), and washed once in Ringer solution containing 0·1 mM phenylmethylsulphonylfluoride and stored at −20 °C. Protein concentration was determined by BCA protein assay reagent according to the procedure provided in the manufacturer's instructions (Pierce).

Immunoblotting

A 30 mg sample of the oocyte homogenate, plasma membrane and vesicles were subjected to SDS electrophoresis in 10% polyacrylamide gel. Electrophoretic fractions were transferred onto a PVDF membrane (Millipore) in 25 mM Tris-HCl, 193 mM glycine and 10% (v/v) methanol, using a Transblot apparatus (Bio-Rad Laboratories). For immunoblotting, the PVDF membranes were incubated in 10% skimmed milk in Tris-buffered saline (TBS), containing 10 mM Tris-HCl (pH 7·4) and 0·9% NaCl), for 2 h at room temperature, washed with 1% skimmed milk and 0·1% Tween-20 in TBS, and then exposed to monoclonal antibodies (all from Chemicon): 1:10 000 mouse anti-actin (which reacts with both G- and F-actin), 1:20 000 mouse anti-tubulin which (reacts with the β subunit of tubulin) and 1:5000 mouse red blood cell (RBC) anti-spectrin (which reacts with the α and β chains of spectrin) in 1% skimmed milk and 0·1% Tween-20 in TBS for 2 h at room temperature. After washing with 1% skimmed milk and 0·1% Tween-20 in TBS, the PVDF membrane was incubated with peroxidase-conjugated anti-mouse IgG at a 1:150 dilution in 1% skimmed milk and 0·1% Tween-20 in TBS for 30 min at room temperature. The immunocomplex was visualized using an enhanced chemiluminescence detection kit (Amersham) following the manufacturer's instructions. Membrane fractions from *Xenopus* RBCs, for testing cross-reactivity between mouse RBC anti-spectrin and *Xenopus* RBC spectrin, were prepared according to Sanchez *et al.* (1990).

Transmission electron microscopy (TEM)

Oocytes and PMV pellets were fixed in a mixture of 1·25% formaldehyde and 2·5% glutaraldehyde, containing 0·03% trinitrophenol and 0·03% $CaCl_2$ in 0·05 M cacodylate buffer (pH 7·3) (Ito & Rikihisa, 1981) overnight, postfixed in 1% OsO_4 in the same buffer, *en bloc* stained with 1% uranyl acetate in 0·1 M maleate buffer (pH 5·2), dehydrated in ethanol and embedded in Poly/Bed 812 (Polysciences). Ultrathin sections were cut on a Reichert Ultracut S ultramicrotome, stained with uranyl acetate and lead citrate and examined in a Philips 201 electron microscope at 60 kV.

Scanning electron microscopy (SEM)

The oocytes and portions of vesicle pellets, after postfixation with OsO_4 for transmission electron microscopy, were separated in different vials and dehydrated in ethanol. Then they were processed through hexamethyldisilazane and air dried. The specimens were mounted on support stubs using high-purity silver paint (SPI Supplies, Structure Probe, Inc., West Chester, PA, USA), sputter coated with gold–palladium alloy for 60 s at 15 mA in a Bal-Tec SCD 004 sputter coater and examined in a Philips 525 M scanning electron microscope at 15 kV.

RESULTS

Hypertonicity induces plasma membrane blebbing of *Xenopus* oocytes

Incubation of *Xenopus* oocytes in hypertonic (~800 mosmol l^{-1}) solution for ~2 h causes extensive plasma membrane blebbing (Fig. 1*A*), with the membrane blebs detaching from the surface of oocytes to become isolated PMVs ranging in size from ~0·5 μm to 20 μm in diameter (Fig. 1*B* and *C*). Individual blebs can be monitored as they grow in size and detach from the surface. Blebs and PMVs examined at the highest optical magnification (× 1500) most often appear as smooth membrane spheres with transparent contents and occasional dark granules that display Brownian motion.

Membrane blebs and PMVs examined with confocal fluorescent microscopy

Confocal fluorescent microscopy was used to examine the cortical cytoskeleton of membrane blebs and vesicles (Fig. 2). Actin and tubulin were labelled with NBD-phallacidin and the DCVJ, respectively. While actin formed a cortical structure directly below the unblebbed plasma membrane, there was no evidence of actin structure in the blebbed membrane (Fig. 2*A* and *C*). In the oocyte shown in Fig. 2*B* and *D*, tubulin did not display a well-defined cortical localization and appeared to be distributed throughout the cytoplasm but was absent from the blebs. In some oocytes, tubulin appeared to be asymmetrically concentrated in the vegetal hemisphere (data not presented; see Gard, 1994, 1999). PMVs were also examined by confocal microscopy for the presence of actin. As shown in Fig. 3, some PMVs showed no evidence of actin-related fluorescence (Fig. 3*A* and *B*) while others showed a low, uniform density of fluorescence (Fig. 3*C* and *D*). This implies that while there may not be a well-defined cortical actin structure, there may be free-floating F-actin in the PMV. Alternatively, one may simply be detecting the stain in the lumen fluid.

We also examined oocytes and PMVs for the presence of spectrin/fodrin using RBC anti-spectrin. Oocytes permeabilized with gluteraldehyde and incubated with mouse RBC anti-spectrin conjugated with fluorescein isothiocyanate (FITC) antibody, display a distinct cortical band around the entire oocyte, thus confirming previous reports that oocytes express spectrin (Giebelhaus *et al.* 1987; Ryabova *et al.* 1994). However, the fluorescent band was too faint, when examined at high magnification, to exclude a low level presence in the bleb (data not presented).

Immunoblot analysis of actin, tubulin and spectrin in cytoplasmic, membrane and PMV fractions

Figure 4*A* shows a Western blot with different lanes containing, homogenate (lane 1), plasma membrane (lane 2) PMVs (lane 3) and 2 μg of actin (lane 4), which were electrophoresed and probed with anti-actin antibody. Figure 4*B* is the same except that the gels were stained with a monoclonal anti-tubulin antibody. Figure 4*C* and *D* are Western blots of purified actin and tubulin proteins detected with anti-actin and anti-tubulin, respectively, and

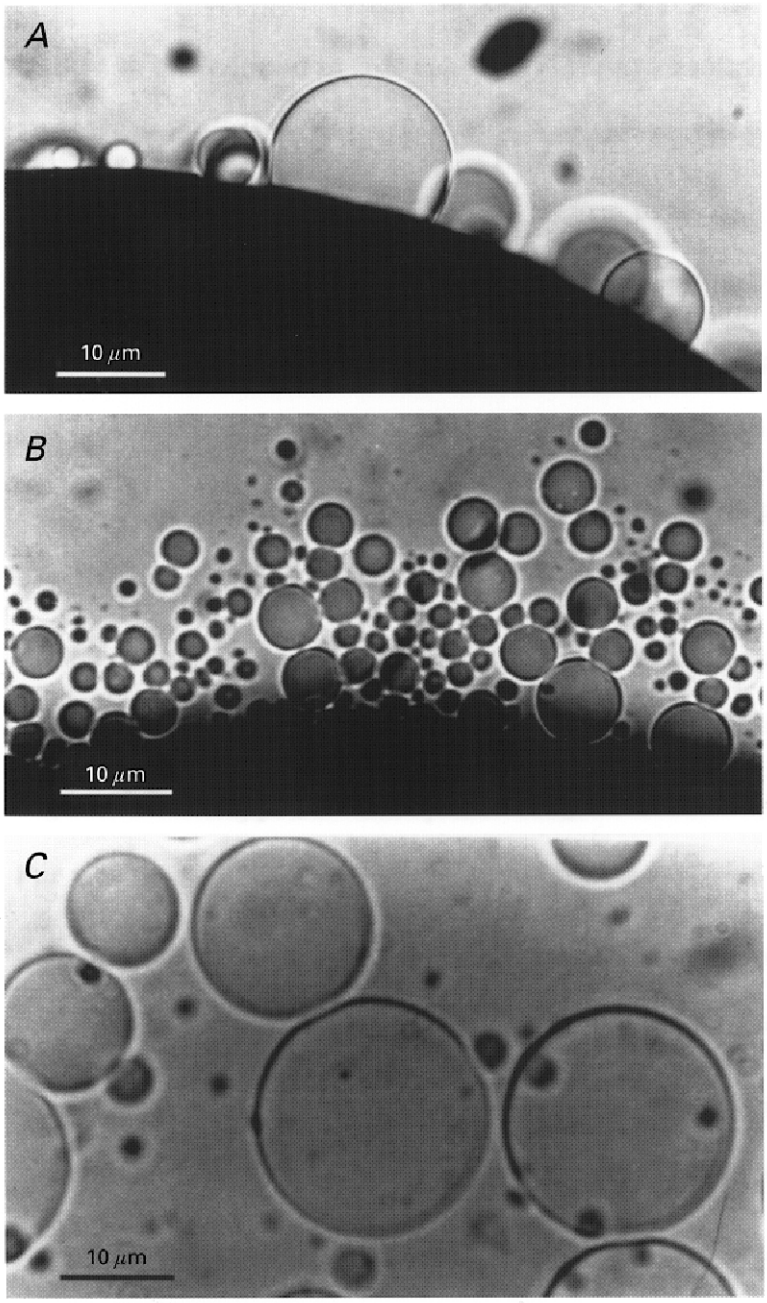

Figure 1. Photomicrographs of hypertonicity-induced plasma membrane blebs and vesicles

A, the blebs appear as transparent membrane blisters on the surface of the oocyte devoid of the pigment granules that darken the cytoplasm of the oocyte. *B*, the focus has been changed to the bottom of the dish and shows the accumulated PMVs. *C*, image of several PMVs showing their spherical shape and optically smooth membrane.

indicate the resolution of the method. The much higher abundance of actin in the homogenate, compared with the membrane fraction, is consistent with reports of high concentrations of free-floating actin monomer (~2 mg ml^{-1}) in the cytoplasm of *Xenopus* oocytes (Merriam & Clark, 1978). In comparison, phallacidin labels F-actin but not G-actin (see Fig. 2*C*). It is not clear why anti-tubulin labels the membrane more strongly than the homogenate, at least based on the DVCJ-labelling pattern in Fig. 2*D*. However, the discrepancy may reflect differential sensitivity of the labels for polymerizing tubulin or sampling differences due to the asymmetrical concentration of tubulin in the vegetal cortex of some oocytes (Gard, 1994)

Western blots stained with mouse RBC anti-spectrin indicate multiple faint bands in the oocyte homogenate and membrane fractions but not in PMV fractions. However, all the bands were smaller than 200 kDa, the molecular mass of spectrin, which we have labelled in *Xenopus* RBC membrane fractions (F. Gao & O. P. Hamill, unpublished observations). These low molecular weight bands may reflect immunologically reactive spectrin fragments generated by proteolysis (see also Giebelhaus *et al.* 1987).

Transmission and scanning electron microscopy of oocytes and PMVs

Transmission EM of control oocytes indicates a highly microvilliated membrane surface with a darkly stained cytoplasm (Fig. 5*A*). In contrast, EM images of PMVs indicate a smooth membrane with relatively low-density flocculent material both inside and outside the vesicle (Fig. 5*B*). Close examination of the vesicle membrane revealed no asymmetry in terms of membrane-associated particles or fibrous material which might otherwise indicate the presence of a cortical cytoskeleton. In comparison, published EM images of RBC membrane show a consistent network-like structure located at the cytoplasmic but not the extracellular membrane face (Tsukita *et al.* 1980). The scanning EM image of the control oocyte (Fig. 5*C*) confirms the high density of microvilli. In contrast, the surface of PMVs appears basically smooth with no evidence of appendages (Fig. 5*D*).

MG channel activity in membrane blebs and vesicles

As indicated in the first paper in this series (Zhang & Hamill, 2000*a*), MG channels are uniformly distributed over the oocyte surface such that all patches show MG channel activity. Similarly, the large majority of patches formed on

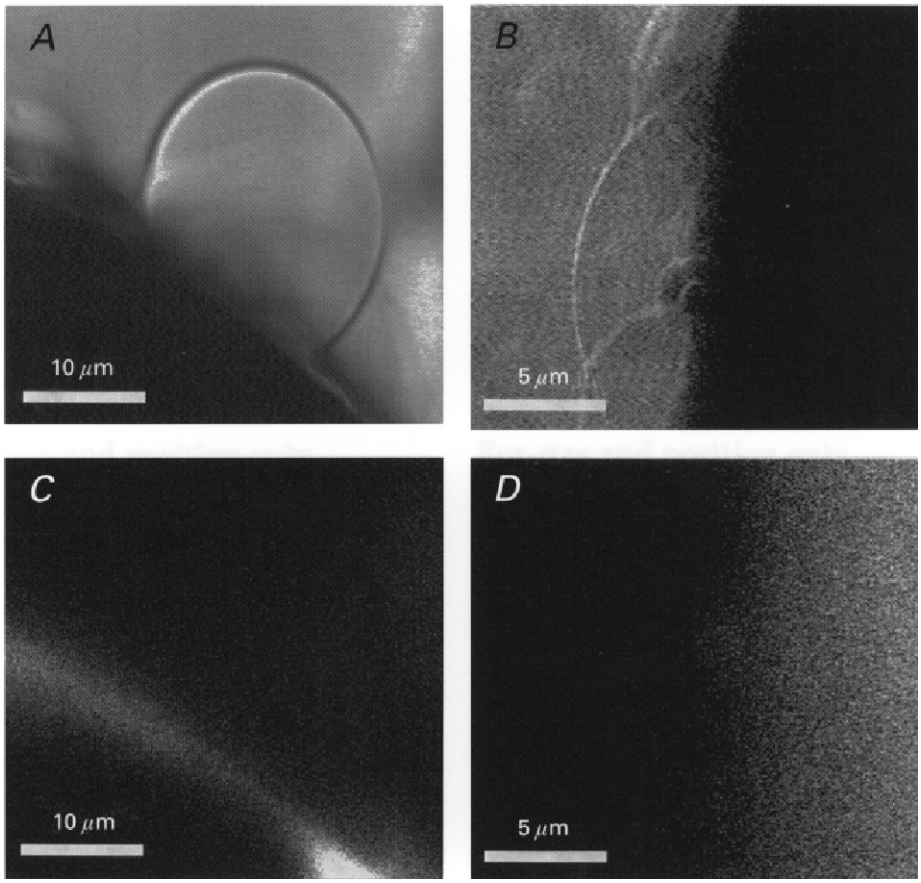

Figure 2. Confocal images showing actin and tubulin distribution in plasma membrane blebs of *Xenopus* oocytes

A and *B*, light images of the blebbed surface of two oocytes. *C*, corresponding fluorescence image for *A* of the NBD-phallacidin-labelled bleb and its parental oocyte. *D*, corresponding fluorescent image for *B* of DCVJ-labelled blebs and their parental oocyte.

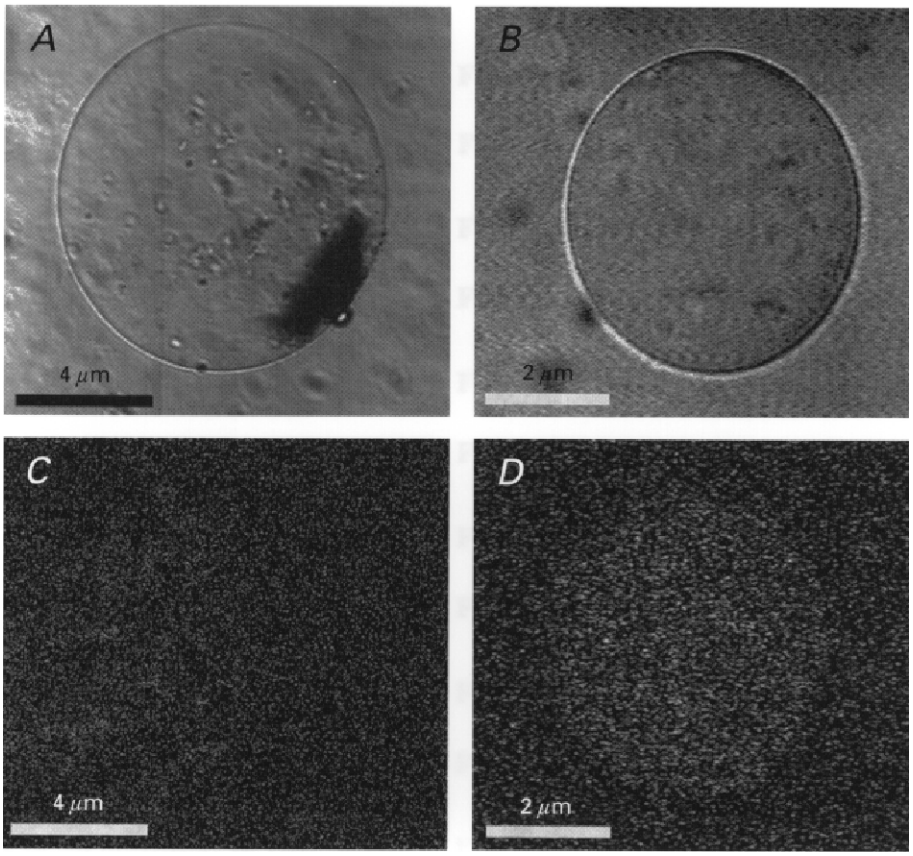

Figure 3. Confocal images of two PMVs from an NBD-phallacidin-labelled oocyte
A and *C*, light images of two different vesicles. *B* and *D*, corresponding fluorescence images of the two vesicles.

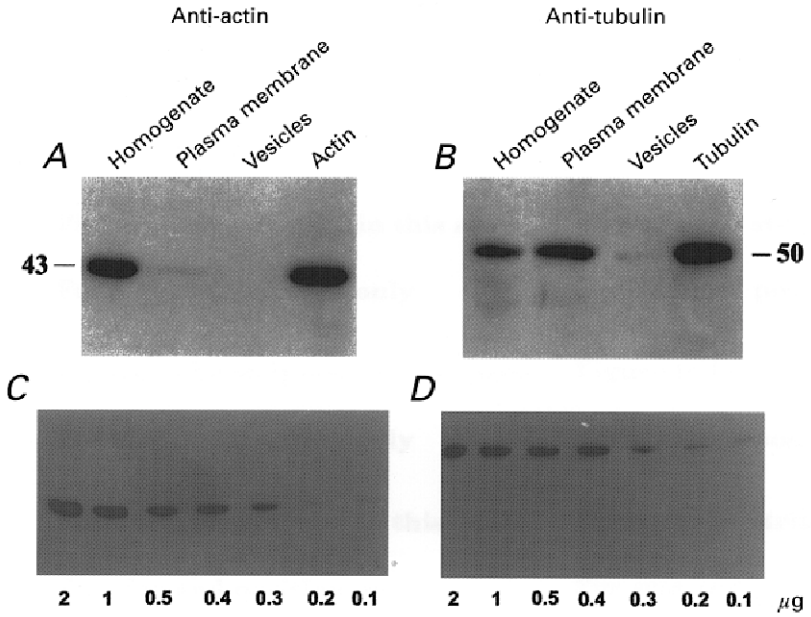

Figure 4. Western blots of homogenate, plasma membrane and vesicles of *Xenopus* oocytes
Actin (*A*) and tubulin (*B*) were labelled with anti-actin and anti-tubulin antibodies, respectively. The resolution limits of the technique were calibrated with different concentrations of actin (*C*) and tubulin (*D*).

blebs and PMVs showed MG channel activity. For example, out of 18 patches formed on blebs, only two failed to show MG channel activity when pressure was increased to the point of causing patch rupture. In the case of PMVs, all 15 patches showed MG channel activity. Note that the presence of MG channel activity on blebs and vesicles formed by hypertonicity contrasts with the frequent absence of MG channel activity on blebs formed by formaldehyde treatment (Zhang *et al.* 1996), possibly indicating that formaldehyde directly inhibits MG channel activity (see Hutter & Williams, 1979).

Recordings of MG channel activities from patches formed on control, bleb and PMV membrane are shown in Fig. 6 (note that the calibration scale for blebs and PMVs is ~10 times control). In the control recordings, after reaching a peak response (6th current trace), the subsequent currents showed large fluctuations in amplitude and adaptation (see also Fig. 7*A*). This variability is a feature of control recordings and may reflect a combination of opposing effects, involving membrane–cytoskeleton decoupling, which reduces the response, and recruitment of new membrane, which increases the response. In comparison, in blebs and PMVs the membrane–cytoskeleton is already decoupled and presumably only membrane recruitment occurs.

The current–pressure relations measured from the recordings in Fig. 6 are shown in Fig. 7*A* and indicate that MG channels in control membrane (again note the response variability after apparent saturation) were initially activated by lower pressures (5 mmHg) than in blebs (15 mmHg) or in PMVs (20 mmHg). The normalized sigmoid curves fitted to the data (Fig. 7*B*) indicate that the pressure for half-maximal MG channel activation was shifted to the right in blebs and PMVs (Fig. 8*A*). This shift would, if anything, be underestimated if the area of patches on blebs and PMVs is larger than the patch area on oocytes (because patches are drawn further up the pipette; see Fig. 10). On the other

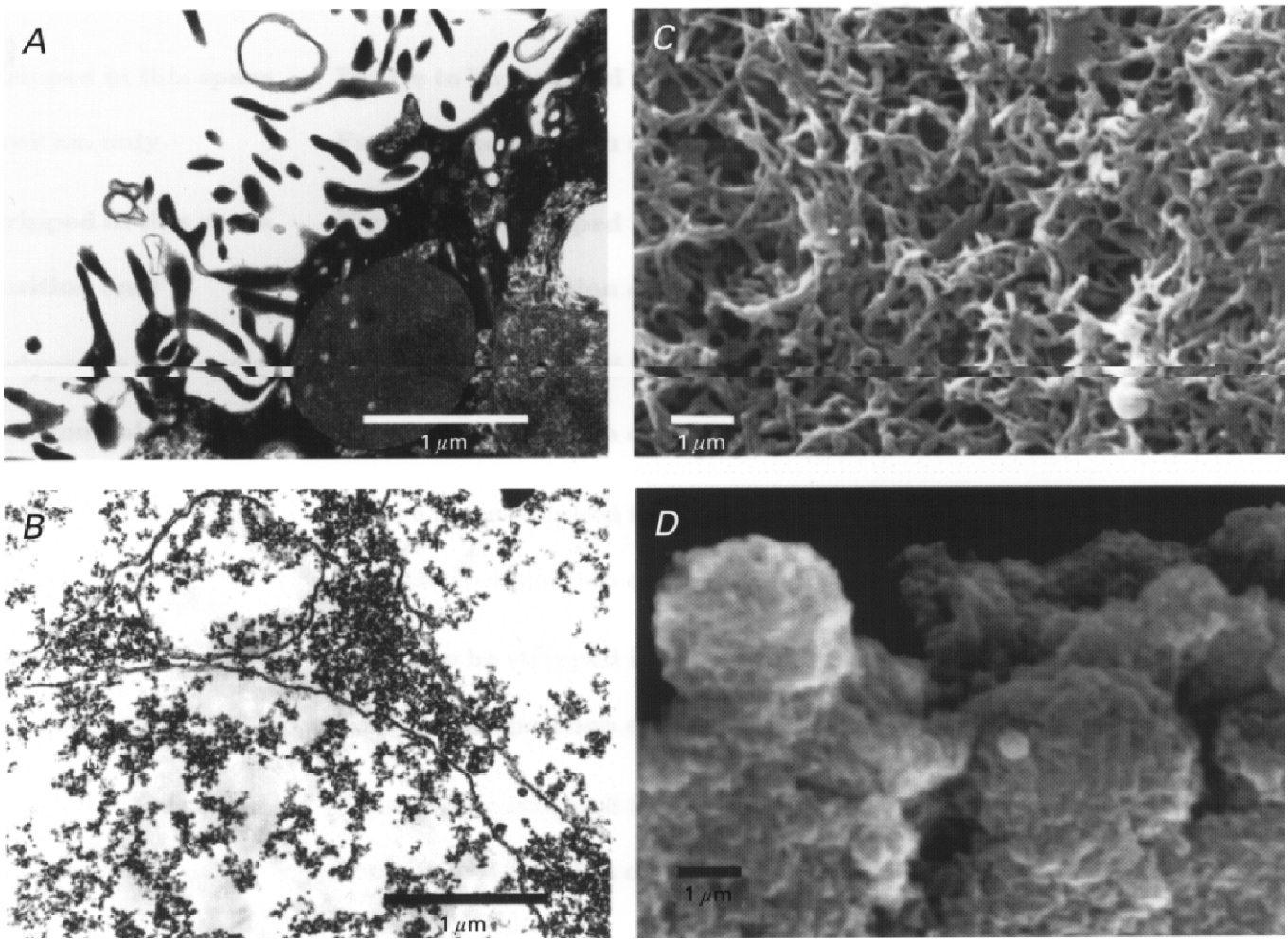

Figure 5. Transmission and scanning electron microscopy of oocyte surface and plasma membrane vesicles

A, TEM of a portion of the oocyte surface showing prominent microvilli containing dark cytoplasmic material. *B*, TEM of PMVs indicating a smooth, even trilaminar membrane, with no evidence of particles or fibres associated with the cytoplasmic side of the membrane. *C*, SEM of the oocyte surface indicating the high density of microvilli. *D*, SEM of PMVs indicating a basically smooth surface membrane with no appendages.

hand, the membrane of blebs and PMVs may have reduced stiffness due to the absence of the cytoskeleton. Such extrinsic factors may underlie the changes in patch mechanosensitivity. Ideally, one would prefer to compare current–tension relations, which would allow for different membrane areas and stiffness under the three conditions. However, high-resolution imaging of bleb and vesicle patches has not yet been carried out. In order to calculate tension from the radius of curvature using Laplace's Law, the membrane material in the patch must remain constant. This condition is least likely to hold during repeated pressure pulses applied to decoupled membrane (see Fig. 10; see also Sokabe *et al.* 1991; Opshal & Webb, 1994*b*).

Whereas MG channel activity in control membrane showed strong adaptation, MG activity in bleb and PMV membrane was sustained for the duration of the pulse. However, the maximal MG channel currents activated at saturating pressures was significantly larger in control than in bleb or PMV membrane (Figs 7*A* and 8*B*). The similar single MG channel current amplitudes (Fig. 9*A* and *B*) and current–voltage relations (Fig. 9*C*) measured in control, bleb and PMV patches show that this difference is not due to significant differences in single-channel conductance.

The above results indicate that the absence of a cortical cytoskeleton removes adaptation and reduces, but does not abolish mechanosensitivity. These changes are similar to those changes observed in cell-attached patches subjected to repeated mechanical stimulation. As illustrated in Fig. 10*A–C*, the membrane patch appears to become decoupled from the underlying cytoplasmic structures (analogous to membrane blebbing), and adaptation and the peak MG current response are reduced (Fig. 10*E* and *F*). In

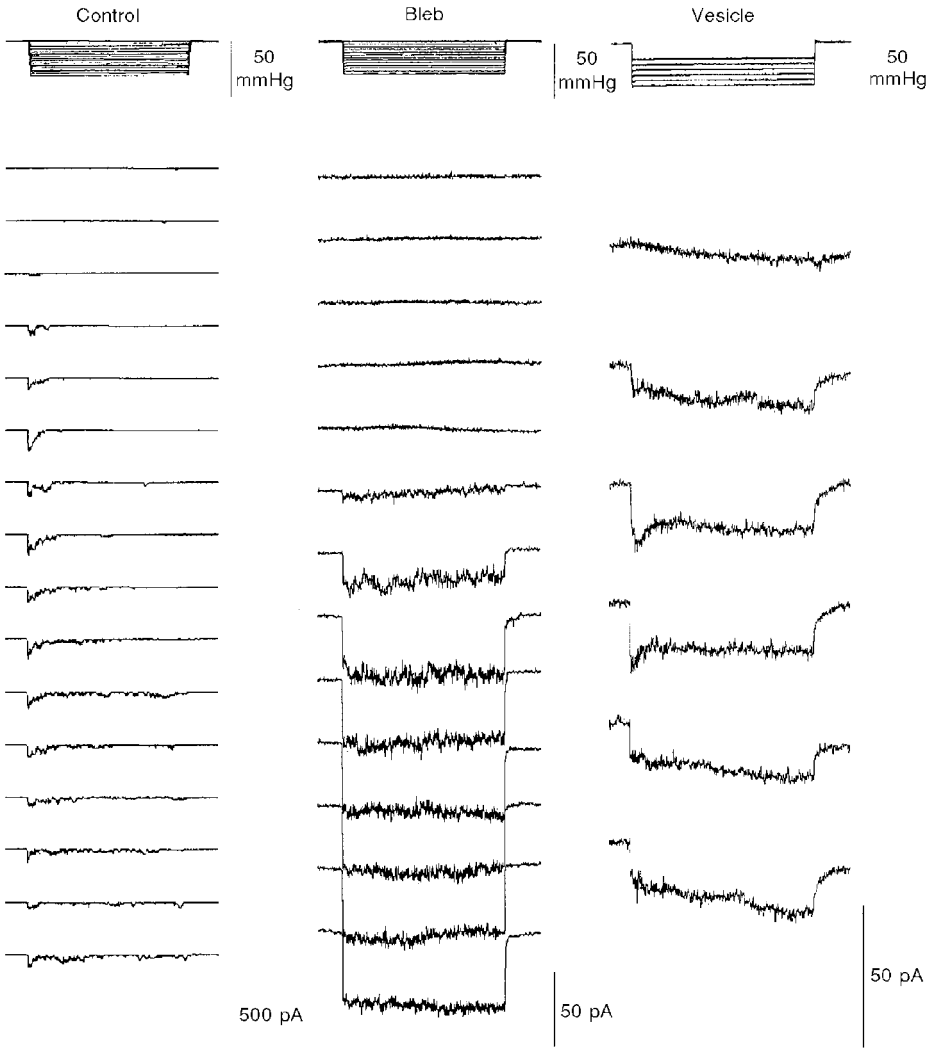

Figure 6. Typical recordings of MG channel activities in membrane patches formed on control, blebbed and vesicular membrane

Incremental pressure pulses of 4 s were applied (upper panel) to activate the current responses shown in the lower panel. The membrane potential in all cases was set at −100 mV (from the measured MG current reversal potential). Note the different current scales in the three conditions.

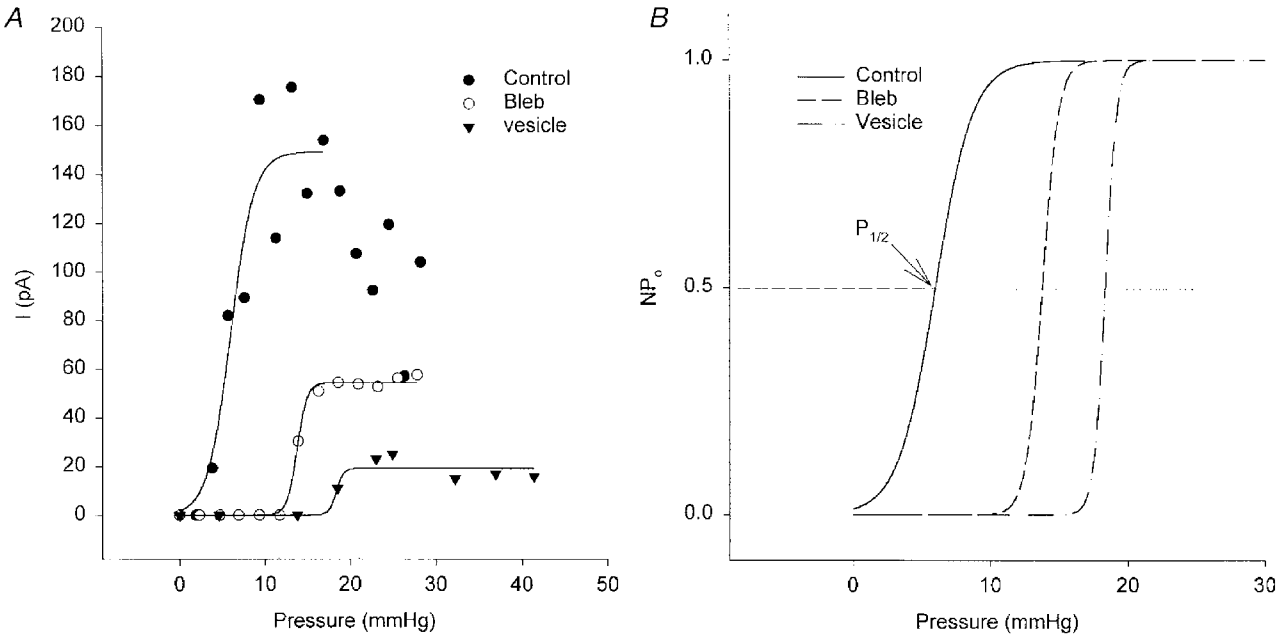

Figure 7. Stimulus–response relations of the MG channels in control, blebbed and vesicular membrane

A, symbols show peak MG channel currents measured from the currents in Fig. 6 as a function of applied pressure. The lines were obtained by fitting these values to Boltzmann relations. *B* shows normalized P_o–pressure relations. As indicated in *B*, half-activation pressure ($P_{1/2}$) represents the pressure at which P_o reaches 0·5.

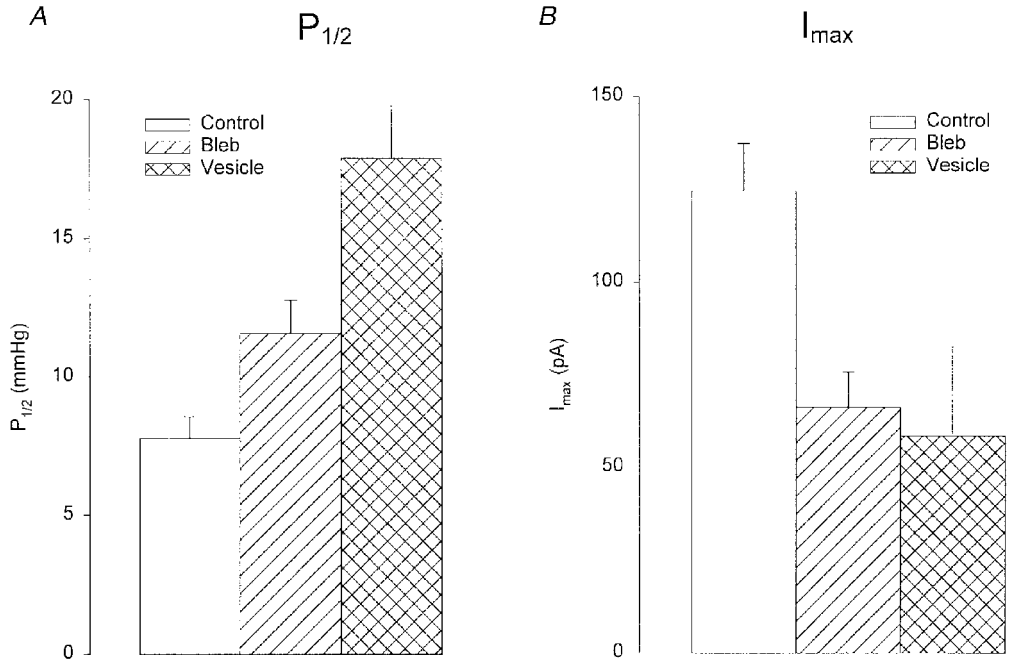

Figure 8. Comparison of mechanosensitivity of MG channels and maximal MG channel currents in membrane patches from control oocytes, blebs and vesicles

The $P_{1/2}$ values (*A*) and maximum current (I_{max}; *B*) were estimated from the Boltzmann relations shown in Fig. 7. The data derives from 15 control patches, 23 bleb patches and 8 vesicle patches. Error bars indicate S.E.M.S. The level of significance for bleb and PMV differences compared with control was either $P < 0{\cdot}01$ or $P < 0{\cdot}05$.

addition, the stimulus–response relation of MG channel activity is shifted to progressively higher pressures (similar to MG activity in blebs and PMVs). Although data from other patches indicate that adaptation can be abolished and MG channel activity more severely reduced than was seen in Fig. 10*F*, we have not observed complete loss of MG activity (while retaining the tight seal), even with more prolonged and stronger stimulation of the patch. This observation contrasts with our earlier observation that MG channel activity could be abolished in some patches (Hamill & McBride, 1992; see Discussion)

Macroscopic MG currents recorded in PMVs

One explanation for the inability to record macroscopic MG channel currents from *Xenopus* oocytes is that the excess plasma membrane, in the form of extensive membrane folds and microvilli, provides an immediate membrane reserve that prevents a bilayer tension increase sufficient to gate the MG channel (Zhang & Hamill, 2000*b*). We therefore predicted that a PMV with its smooth membrane and spherical geometry would require only slight inflation to activate whole-vesicle MG channel currents. In order to reduce the common occurrence of pressure-induced rupture of the PMVs (expected with 2–4% inflations), we studied relatively small vesicles (~10 μm diameter). According to Laplace's Law, smaller PMVs should tolerate larger pressures before rupturing. Figure 11 shows a single experiment in which we obtained both cell-attached patch and whole-vesicle recordings from the same PMV. This vesicle was ~10 μm in diameter, which would give a total membrane area of ~300 μm^2, and can be compared with the estimated area of the cell-attached patch of ~10 μm^2 in our standard pipettes with an internal tip diameter of 2 μm (Zhang & Hamill, 2000*a*). As shown in Fig. 11, suction steps

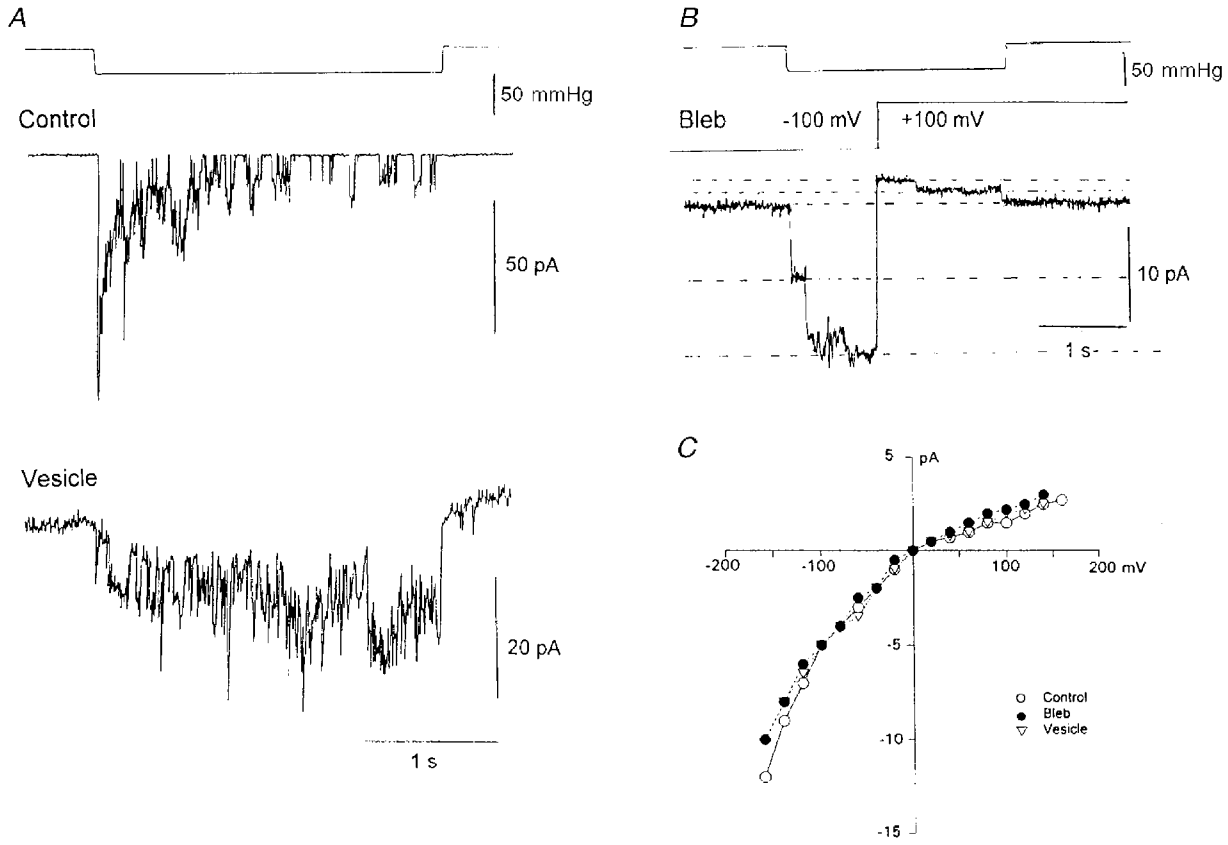

Figure 9. Single MG channel current behaviour in control, vesicle and bleb membrane

A, the current response to identical suction steps in cell-attached patches on an oocyte and a vesicle. Patch potential was set to give a −150 mV driving force (from the reversal potential of the MG current). The single-channel current amplitudes in control oocytes and PMVs were 12 and 10 pA, respectively. The two recordings were made with pipettes from a single capillary pull to ensure identical pipette tip dimensions. Note the typical noisy background vesicle current. *B*, demonstration of the strong rectification of MG channelscurrents recorded on a membrane bleb. While the suction step was maintained (top trace) the voltage was switched from −100 mV (8 pA) to +100 mV (1·6 pA). The current transient associated with the voltage step was removed by subtraction using a current trace with no applied pressure step. *C*, current–voltage relations measured on control, bleb and vesicle membranes. The data points are the mean of 5–10 individual MG channel currents measured directly from the oscilloscope screen at different voltages. The data were shifted to give a reversal potential of ~0 mV. The pipette solution in all recordings contained 100 mM KCl and 5 mM K-Hepes.

applied to the patch activated MG channel activity and gave a maximal current of ~25 pA. After patch rupture and formation of the whole-vesicle configuration, pressure steps reversibly activated currents with an amplitude of ~400 pA. Presumably this was close to the maximal current since the vesicle ruptured during the same pressure step. These results indicate that the maximal whole-vesicle current was within a factor of 2 of the MG currents anticipated from patch recordings. The pressures required to rupture the patch (~50 mmHg) and the whole vesicle (~12 mmHg) are qualitatively consistent with predictions based on Laplace's Law. In five other PMVs in which successful whole-vesicle recordings were achieved (~5% of attempts) similar behaviour with pressure-activated currents of 300–700 pA were recorded. In all cases, the currents turned off rapidly (within 100 ms) with the pressure step. Such kinetic behaviour is more consistent with MG channels than reversible breakdown of the vesicle membrane. Furthermore, when recordings were made in 20 μM Gd^{3+}, the vesicles ruptured without prior activation of pressure-sensitive currents (2 PMVs, data not shown).

DISCUSSION

In this study we describe a novel method for causing the *Xenopus* oocyte to bleb and shed membrane vesicles. The method, which involves exposure of oocytes to hypertonic solution, offers a number advantages over previous methods used to isolate plasma membrane. First, our method does not require the introduction of foreign chemicals (e.g. aldehydes) typically used to cause membrane blebbing (Scott, 1975; Scott *et al.* 1979; Hamill *et al.* 1995). Thus we avoid the possible alteration of membrane proteins and lipids by such chemicals (Hutter & Williams, 1979). Second, the method does not require homogenization or disruption of the oocyte and therefore reduces the likelihood that PMVs are

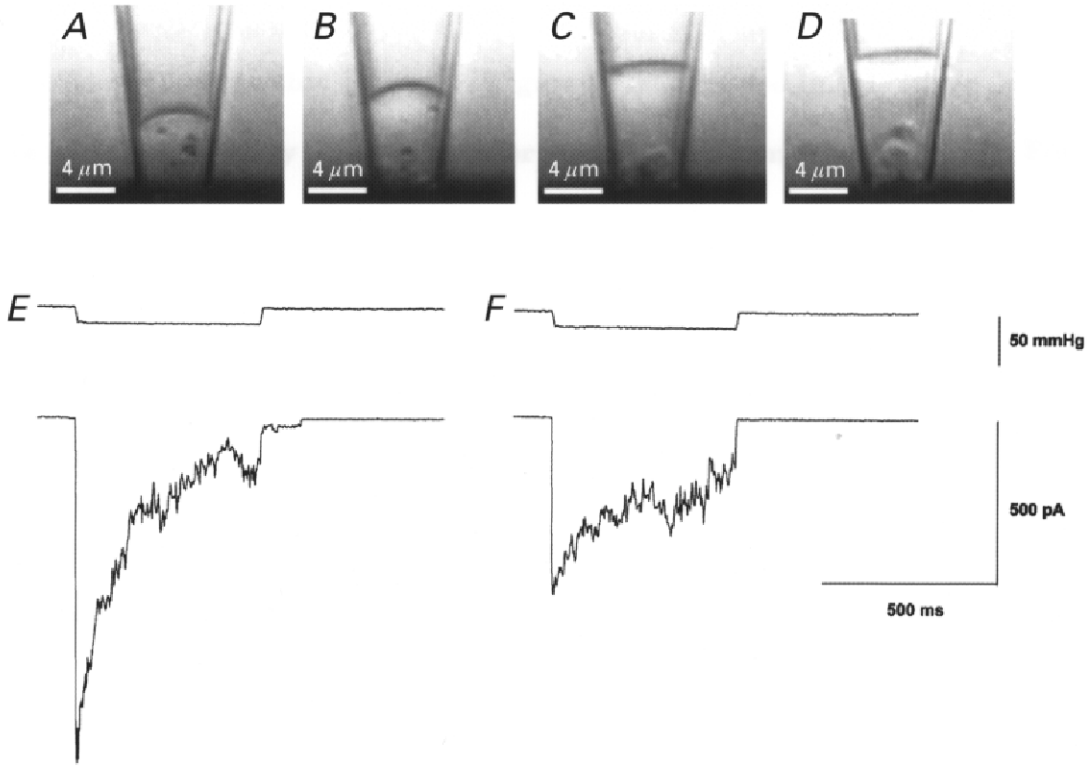

Figure 10. Images and MG current recordings of a membrane patch in response to repetitive mechanical stimulation

The top panels (*A–D*) show video images of a cell-attached patch at different times after the formation of the tight seal and the bottom panels (*E* and *F*) show the current response at the time of image *A* and *D*, respectively. Between each image, short (100 ms) suction and pressure step protocols were applied (not shown). *A*, the first image taken soon after seal formation shows the patch slightly curved and located close (~5 μm) to the cell surface. Particles located in the cytoplasm displayed no motion presumably because they were immobilized on cytoskeleton structures. *B–D*, with repetitive stimulus protocols, the patch progressively moved up the pipette away from the cell and a clear space (most evident in *D*) developed between the membrane and cytoskeleton structures remaining close to the cell. Cytoplasmic particles that moved into this clear space displayed Brownian motion indicating the absence of constraining structures (see also Sokabe & Sachs, 1990). *E*, application of a pressure pulse at the time of image *A* caused a rapid increase in MG channel activity that then adapted (i.e. closed) in the presence of sustained stimulation. *F*, application of the same pressure pulse at the time of image *D* caused activation of a smaller response that showed reduced adaptation. The patch pipette tip diameter was ~4 μm.

contaminated by intracellular membranes and organelles (Wall & Patel, 1989). Third, the PMVs are sealed right side out so that membrane proteins are in their proper orientation. Finally, the method is simple, relatively fast and provides a good yield of PMVs from as few as 100 cells. We believe this method should prove useful for future biochemical analysis of both endogenous membrane proteins and foreign proteins heterologously expressed in *Xenopus* oocytes.

The mechanism by which hypertonicity causes oocyte blebbing is not clear. In fact, we were surprised by the effect because we had initially tried hypotonicity with no success, and yet this treatment is known to cause muscle fibre blebbing (Zollinger, 1947). It may be that hypertonicity, by shrinking the oocyte, further increases the excess membrane area, thereby destabilizing the bilayer and causing membrane vesiculation. Another possible mechanism may be related to the large non-selective current (I_{shrink}) which is activated by hypertonicity (Zhang & Hamill, 2000*a*). The associated ionic fluxes may either directly or indirectly (e.g. by ATP depletion) destabilize or depolymerize the cortical cytoskeleton and in this way promote vesiculation. Further experiments will be required to discriminate between the possible mechanisms.

The most common mechanism evoked to explain blebbing in mammalian cell lines is that the plasma membrane, once decoupled from its underlying cytoskeleton, becomes susceptible to pressurization by hydrostatic forces generated within the cell (Scott *et al.* 1979). Since in the oocyte one can follow, over a few minutes, the growth of individual membrane blebs and their detachment from the oocyte, it would seem that oocyte blebs and vesicles also derive from decoupled plasma membrane. However, recent evidence indicates that the oocyte plasma membrane normally undergoes an extremely high rate of turnover (complete turnover within 24 h) involving equal rates of exocytosis and endocytosis (Zampighi *et al.* 1999). In this case, it may be that disruption of this normally balanced process can also contribute to membrane blebbing.

EM studies of membrane blebs formed on mammalian cells indicate a membrane with a simple trilaminar structure (i.e. devoid of a cortical cytoskeleton) enclosing a structureless cytoplasm (Scott, 1975; Scott *et al.* 1979). Our EM images of *Xenopus* oocyte PMVs are also consistent with this view. In particular, EM images of oocyte PMVs support our immunocytochemical studies, which indicate a deficiency of cortical cytoskeleton proteins in PMV fractions. In the specific case of spectrin, others have shown, with immunofluorescence, that spectrin is localized in the oocyte cortex (see Ryabova *et al.* 1994). However, our EM images of PMV membrane show no evidence of an associated 'spectrin-like' cytoskeleton network like that so clearly resolved in EM

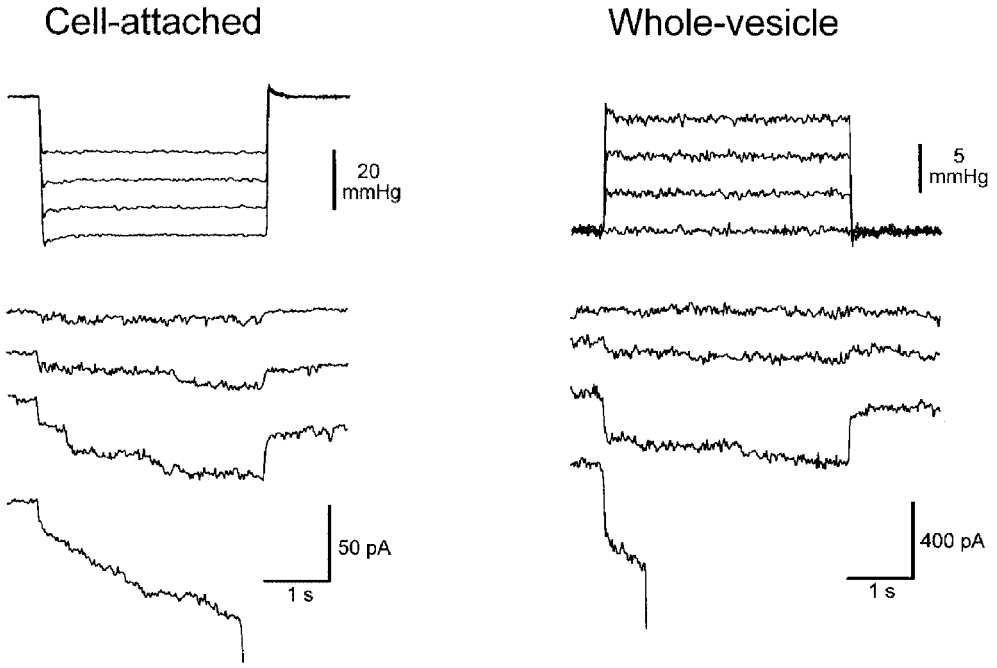

Figure 11. Recordings of mechanosensitive currents from a cell-attached patch and from the same whole vesicle

The membrane potential was held at −50 mV for both configurations (pipette potentials were +50 and −50 mV for the cell-attached patch and the whole vesicle, respectively). Left, MG channel activity in response to incrementing suction 4 s duration pulses that ultimately ruptured the patch. Right, MS currents in whole-cell configuration in response to incrementing 4 s duration pressure pulses applied to inflate the vesicle. The whole vesicle mechanosensitive current activated in the 3rd current trace turned off rapidly with the pressure step. The last pressure step activated the MS current but after a delay also ruptured the vesicle. Note the different pressure and current scales.

images of RBC membrane (see Fig. 2a of Tsukita *et al.* 1980).

The main results of this study indicate that MG channels can still be activated in plasma membrane that is deficient in cytoskeleton structures and proteins. The single MG channels recorded on blebs and PMVs display the same single-channel conductance and I–V relation seen on control membrane. However, the channel activity differs from the MG channel activity seen on gently sealed oocyte patches in that it shows reduced adaptation and mechanosensitivity. On the other hand, it is similar to MG activity seen after mechanical over-stimulation of the oocyte patch (Fig. 10). These results support the idea that membrane–cytoskeleton interactions may be mechanically disrupted in the patch leading to reduced adaptation and mechanosensitivity (Hamill & McBride, 1992). In this case, these changes most probably involve extrinsic factors (e.g. membrane stiffness), which determine how mechanical energy is conveyed to the channel protein, rather than changes in the intrinsic properties of the channel protein.

The activation of MG channels in the apparent absence of cytoskeleton structures has a number of important implications regarding the gating mechanism of the oocyte MG channel. In the past, two basic models of MG channel gating have been proposed. In one model, referred to as the bilayer model, the channel is gated by tension developed purely in the bilayer. This model most probably explains the mechanosensitivity of specific prokaryotic MG channels (Martinac *et al.* 1990; Sukahrev *et al.* 1997), as well as the simple channel forming peptides alamethicin and gramicidin, which express mechanosensitivity in pure lipid bilayers (Opshal & Webb, 1994*a*; Goulian *et al.* 1998). In the second model, referred to as the tethered model, the channel is gated by tension developed in extracellular or cytoskeleton structures coupled to the channel protein. This model has been proposed to explain the mechanosensitivity of a variety of eukaryotic channels (Corey & Hudspeth, 1983; Guharay & Sachs, 1984). However, the evidence for this model is not as strong and mainly comes from observations that disruption of extracellular or cytoskeleton elements can abolish or reduce mechanosensitivity (Assad *et al.* 1991). For example, the tethered model has been used to explain the loss or reduction of oocyte MG channel activity reported by Hamill & McBride (1992). In this early study, MG channel activity was completely abolished in some patches. However, we have not been able to reproduce this effect in subsequent studies (see Fig. 10). The reason for the original observation may be that mechanical stimulation of the pipette can cause patch excision and result in closed vesicle formation in the pipette. Under these conditions the channel currents may be severely attenuated by flow through the series resistance combination of the vesicle (see Hamill *et al.* 1981). On the other hand, the present results showing that MG channel activity is retained in cytoskeleton deficient PMVs may indicate that the bilayer model applies to at least oocyte MG channel activation, with the cytoskeleton playing some role in modulating adaptation kinetics and mechanosensitivity. For example, rapid adaptation may reflect load bearing (viscous) elements in the cortical cytoskeleton that can reorganize themselves and thereby relax tension in the bilayer, (Hamill & McBride, 1994). When these elements are disrupted, membrane tension is maintained for the duration of the stimulus. Similarly, the cortical cytoskeleton may also act to increase the mechanosensitivity of the patch by constraining the lipid bilayer, thereby impeding rapid fluid flow in response to stimulation (see Fig. 10).

Recently, studies of a number of other eukaryotic MG channels indicate that the bilayer rather than the tethered model may also provide a better explanation of their mechanosensitivity (Casado & Ascher, 1998; Patel *et al.* 1998). However, the ultimate proof of a bilayer-type mechanism for any MG channel (including the oocyte channel) requires protein purification and demonstration of mechanosensitivity when reconstituted into lipid bilayers (Sukharev *et al.* 1997). In this case, our method of forming cytoskeleton-deficient PMVs that clearly retain MG channel activity may facilitate the first step in the purification and possible reconsitution of eukaryotic MG channel proteins.

In contrast to our inability to activate whole-oocyte MG currents by inflation (Zhang & Hamill, 2000*b*), we were able to reversibly activate currents by pressure inflation of PMVs. This observation is consistent with our hypothesis that the excess membrane area of the oocyte, in the form of extensive membrane folds and microvilli, prevents the development of membrane tension that would otherwise activate MG channels but also run equal risk of damaging the oocyte membrane. In comparison, the isolated PMV displays a smooth spherical geometry such that the slightest inflation (1–4 % and below detection limits) results in either MG current activation or vesicle rupture.

We have already discussed how membrane geometry of specific cell types may play a role in determining the mechanosensitive response of cells (Zhang & Hamill, 2000*b*). Another issue is whether bleb formation, by smoothing out excess membrane area, may modify the cell mechanosensitivity. Although blebs were originally described in cells stressed by various experimental treatments, membrane blebbing can also occur in uninjured cells during various physiological processes including cell spreading (Ericksen & Trinkaus, 1976), cell movements (Trinkaus, 1980), mitosis (Porter *et al.* 1973) and programmed cell death or apoptosis (Kerr *et al.* 1972). If MG channels are localized in such membrane blebs, their mechanosensitivity may be unmasked by the blebbing process so that they play some signalling role in these cellular functions.

Conclusions

The results of these three papers have focused on the *Xenopus* oocyte MG channel, which has been extensively studied in patch-clamp recordings and revealed a number of interesting but as yet unexplained biophysical phenomena.

Our results indicate that membrane area redundancy, an adaptation probably found in all animal cells that allows for cell deformations and cell motions without stressing the membrane bilayer, may also serve to prevent the activation of MG channels in the whole cell. We demonstrate that, under specific conditions when membrane geometry is simplified either by the process of tight seal patch formation or membrane blebbing, the bilayer may be subject to tension changes that activate MG channels. We propose that differences in membrane geometry within a single cell or changes in membrane geometry that occur during physiological, developmental or pathological conditions may modify the mechanosensitive response of the cell independently of the intrinsic properties of the membrane proteins.

Assad, J. A., Shephard, G. M. G. & Corey, D. P. (1991). Tip link integrity and mechanical transduction in vertebrate hair cells. *Neuron* **7**, 985–994.

Casado, M. & Ascher, P. (1998). Opposite modulation of NMDA receptors by lysophospholipids and arachidonic acid: common features with mechanosensitivity. *Journal of Physiology* **513**, 317–330.

Corey, D. P. & Hudspeth, A. J. (1983). Kinetics of the receptor current in bullfrog saccular hair cells. *Journal of Neuroscience* **3**, 962–976.

Erikson, C. A. & Trinkaus, J. P. (1976). Microvilli and blebs as sources of reserve surface membrane during cell spreading. *Experimental Cell Research* **99**, 375–384.

Gard, D. L. (1994). γ-Tubulin is asymmetrically distributed in the cortex of *Xenopus* oocytes. *Developmental Biology* **161**, 131–140.

Gard, D. L. (1999). Confocal microscopy and 3-D reconstruction of the cytoskeleton of *Xenopus* oocytes. *Microscopy Research and Technique* **44**, 388–414.

Giebelhaus, D. H., Zelus, B. D., Henchman, S. K. & Moon, R. T. (1987). Changes in the expression of α-fodrin during embryonic development of *Xenopus laevis*. *Journal of Cell Biology* **105**, 843–853.

Goulian, M., Mesquita, O. N., Fygenson, D. K., Nielsen, C., Andersen, O. S. & Libchaber, A. (1998). Gramicidin channel kinetics under tension. *Biophysical Journal* **74**, 328–337.

Guharay, F. & Sachs, F. (1984). Stretch-activated single ion channel currents in tissue-cultured embryonic chick skeletal muscle. *Journal of Physiology* **352**, 685–701.

Hamill, O. P., Chen, M., Zhang, Y. & McBride, D. W. Jr (1995). A cytoskeleton (CSK) deficient plasma membrane vesicle preparation from *Xenopus* oocytes for studying CSK effects on membrane ion channel gating. *Journal of Physiology* **483.P**, 162*P*.

Hamill, O. P. & McBride, D. W. Jr (1992). Rapid adaptation of single mechanosensitive channels in *Xenopus* oocytes. *Proceedings of the National Academy of Sciences of the USA* **89**, 7462–7466.

Hamill, O. P. & McBride, D. W. Jr (1994). Molecular mechanisms of mechanoreceptor adaptation. *News in Physiological Sciences* **9**, 53–59.

Hamill, O. P. & McBride, D. W. Jr (1997). Induced membrane hypo/hyper-mechanosensitivity: a limitation of patch-clamp recording. *Annual Review of Physiology* **59**, 621–631.

Hamill, O. P., Marty, A., Neher, E., Sakmann, B. & Sigworth, F. J. (1981). Improved patch-clamp techniques for high-resolution current recording from cells and cell-free membrane patches. *Pflügers Archiv* **391**, 85–100.

Hutter, O. F. & Williams, T. L. (1979). A dual effect of formaldehyde on the inwardly rectifying potassium conductance in skeletal muscle. *Journal of Physiology* **286**, 591–606.

Ito, S. & Rikihisa, Y. (1981). Techniques for electron microscopy of rickettsiae. In *Rickettsiae and Rickettsial Deseases*, ed. Burgdorfer, W. & Anacker, R. L., pp. 213–227. Academic Press, New York.

Kerr, J. F. R., Wiley, A. H. & Currie, A. R. (1972). Apoptosis: a basic phenomenon with wide ranging implications in tissue kinetics. *British Journal of Cancer* **26**, 239–357.

Martinac, B., Adler, J. & Kung, C. (1990). Mechanosensitive ion channels of E. coli activated by amphipaths. *Nature* **348**, 261–263.

Merriam, R. W. & Clark, T. G. (1978). Actin in *Xenopus* oocytes. II. Intracellular distribution and polymerizability. *Journal of Cell Biology* **77**, 439–447.

Morris, C. E. & Horn, R. (1991). Failure to elicit neuronal macroscopic mechanosensitive currents anticipated by single-channel studies. *Science* **251**, 1246–1249.

Opsahl, L. & Webb, W. W. (1994*a*). Transduction of membrane tension by the ion channel alamethicin. *Biophysical Journal* **66**, 71–7.

Opsahl, L. & Webb, W. W. (1994*b*). Lipid-glass adhesion in giga-sealed patch-clamped membranes. *Biophysical Journal* **66**, 75–79.

Patel, A. J., Honore, E., Maingret, F., Lesage, F., Fink, M., Duprat, F. & Lazdunski, M. (1998). A mammalian two-pore domain mechano-gated S-like K^+ channel. *EMBO Journal* **17**, 4283–4290.

Porter, K. R., Prescott, D. & Frye, J. (1973). Changes in the surface morphology of Chinese hamster cells during the cell cycle. *Journal of Cell Biology* **57**, 815–836.

Ryabova, L. V., Virtanen, I., Wartiovaara, J. & Vassetzky, S. G. (1994). Contractile proteins and nonerythroid spectrin in oogenesis of *Xenopus laevis*. *Molecular Reproduction and Development* **37**, 99–109.

Sanchez, I., Twersky, L. H. & Cohen, W. D. (1990). Detergent based isolation of marginal bands of microtubules from nucleated erythrocytes. *European Journal of Cell Biology* **52**, 349–358.

Scott, R. E. (1975). Plasma membrane vesiculation: A new technique for isolation of plasma membranes. *Science* **194**, 743–745.

Scott, R. E., Perkins, R. G., Zschunke, M. A., Hoerl, B. J. & Maercklein, P. B. (1979). Plasma membrane vesiculation in 3T3 and SV3T3 cells. I. Morphological and biochemical characterization. *Journal of Cell Science* **35**, 229–243.

Sokabe, M. & Sachs, F. (1990). The structure and dynamics of patch-clamped membranes: a study using differential interference contrast light microscopy. *Journal of Cell Biology* **111**, 599–606.

Sokabe, M., Sachs, F. & Jing, Z. (1991). Quantitative video mocroscopy of patch clamped membranes stress, strain, capacitance and stretch channel activation. *Biophysical Journal* **59**, 722–728.

Small, D. L. & Morris, C. E. (1994). Delayed activation of single mechanosensitive channels in Lymnaea neurons. *American Journal of Physiology* **267**, C598–606.

Sukharev, S. I., Blount, P., Martinac, B. & Kung, C. (1997). Mechanosensitive channels of *Escherichia coli*: the MscL gene, protein, and activities. *Annual Review of Physiology* **59**, 633–657.

Trinkhaus, J. P. (1980). Formation of protrusions of the cell surface during cell movement. *Progress in Clinical Biological Research* **41**, 887–906.

Tsukita, S., Tsukita, S. & Ishikawa, H. (1980). Cytoskeletal network underlying the human erythrocyte membrane. *Journal of Cell Biology* **85**, 567–576.

Wall, D. A. & Patel, S. (1989). Isolation of plasma membrane complexes from *Xenopus* oocytes. *Journal of Membrane Biology* **107**, 189–201.

Wan, X., Juranka, P. & Morris, C. E. (1999). Activation of mechanosensitive currents in traumatized membrane. *American Journal of Physiology* **276**, C318–327.

Zampighi, G. A., Loo, D. D. F., Kreman, M., Eskandari, S. & Wright, E. M. (1999). Functional and morphological correlates of connexin50 expressed in *Xenopus laevis* oocytes. *Journal of General Physiology* **113**, 507–523.

Zhang, Y., McBride, D. W. Jr & Hamill, O. P. (1996). On the nature of mechano-gated channel activity in cytoskeleton deficient vesicles shed from *Xenopus* oocytes. *Biophysical Journal* **70**, A349.

Zhang, Y. & Hamill, O. P. (2000*a*). Calcium-, voltage- and osmotic stress-sensitive currents in *Xenopus* oocytes and their relationship to single mechanically gated channels. *Journal of Physiology* **523**, 83–99.

Zhang, Y. & Hamill, O. P. (2000*b*). On the discrepancy between whole-cell and membrane patch mechanosensitivity in *Xenopus* oocytes. *Journal of Physiology* **523**, 101–115.

Zollinger, H. U. (1947). Cytologic studies with the phase microscope. I. The formation of 'blisters' on cells in suspension (potocytosis), with observations on the nature of the cellular membrane. *American Journal of Pathology* **24**, 545–567.

Acknowledgements

Our research is supported by the National Institute of Arthritis and Musculoskeletal and Skin Diseases (Grant R01-AR42782) and the Muscular Dystrophy Association.

Corresponding author

O. P Hamill: Physiology and Biophysics, University of Texas Medical Branch, Galveston, TX 77555-0641, USA.

Email: ohamill@utmb.edu